Design of Dielectric Waveguide Bandpass Filters Using Parallel-Coupled Gratings

PERTTI K. IKÄLÄINEN, STUDENT MEMBER, IEEE, AND GEORGE L. MATTHAEI, FELLOW, IEEE

Abstract—**Techniques for the design of narrow-band (of the order of a percent or so), bandpass filters using dielectric waveguide gratings are presented. These filters use both single, uncoupled gratings and parallel-coupled configurations of gratings to form multiresonator bandpass filter structures. Transmission-line equivalent circuits are used to model the dielectric waveguide gratings. Using this model, it is then shown how direct-coupled-resonator theory can be applied to such filter structures to synthesize a prescribed passband having Chebyshev or maximally flat characteristic. On the other hand, the parallel-coupled gratings give these filters broad and strong, absorptive stopbands, as is explained. Experimental results are presented which show good agreement between theoretical and measured results.**

I. Introduction

DIELECTRIC WAVEGUIDES are potentially attractive for use in millimeter-wave and optical integrated circuits. Over the years a number of different configurations of dielectric waveguide (DW) have been proposed, and their waveguiding properties have been studied. However, so far relatively few practical techniques have been established for the design of components using DW, especially filters. The purpose of this study has been to investigate means for bandpass filter design using DW gratings. The design of bandpass filters in DW has been hampered by the fact that in most cases, the energy guided by a DW is loosely bound to the guide, and therefore conventional forms of resonators usually cannot be used because radiation occurs at all abrupt discontinuities with a consequent degradation in resonator Q. One approach that has been used is the ring resonator filter [1]. However, it has a serious drawback in that in order to avoid radiation losses, the ring has to be many wavelengths in circumference which results in closely spaced, spurious passbands. The problems associated with radiation in the passband have been avoided in filters designed using "nonradiative" dielectric waveguide where the dielectric is confined between two, parallel, closely spaced metal planes [2]. These filters have shown good passband performance but broad, strong stopbands may be difficult to achieve because, at frequencies for which the spacing between the plates exceeds one half-wavelength in air, the guide is no longer in the "nonradiative" regime of operation.

DW gratings have well-known applications as bandstop filters [3], [4]. For bandpass filters, they can be used in pairs on a single guide (a type of Fabry–Perot resonator) or in a parallel-coupled configuration. The first approach is of limited practicality as a bandpass filter because the stopband width is, in most cases, less than 10 percent. The latter approach yields particularly good stopband behavior, and we have previously discussed the design of simple bandpass filters using parallel-coupled gratings [5]. In [5], we also demonstrated a coupled-resonator filter which used both single, uncoupled gratings and parallel-coupled gratings, and we were able to obtain a trial design with a Chebyshev passband along with broad, absorptive stopbands. However, at that time, general design theory for such filters had not been explored. It is the purpose of this paper to present our more recent results for filters of this class and to present practical design procedures for such filters. These filters appear to be best suited for narrow bandwidth applications where broad, strong stopbands are necessary. If broader passband bandwidths are desired, then the use of DW bandstop filters together with a 3-dB coupler [4] may be considered.

II. Modeling of DW Gratings

In our experiments we have used image guide DW, though doubtlessly other forms of DW could also be used with these techniques. We formed the gratings by cutting notches in the sides of the image guide, which was found to be preferable when the vertically polarized lowest order mode is used [6] (this mode would be called E_{11}^{y} in the notation of [7]). Such a grating is shown schematically in Fig. 1(a). We have found that their frequency response can be accurately modeled, at least in the vicinity of the stopband, with a transmission-line equivalent circuit, Fig. 1(b), in which all the line segments are specifically of the same length. While we endeavored to make the electrical lengths of the notched and unnotched regions of the grating approximately equal, it is not a necessary condition for the equivalent circuit of Fig. 1(b) to apply. Discontinuity fringing field effects are not ignored, as a measured center frequency and an *effective* impedance ratio are used to characterize a given grating. Center frequency f_0' is defined as the stopband center frequency. For Fig. 1(b), it is the frequency for which all line segments are a quarter-wave-

Manuscript received August 26, 1985; revised December 20, 1985. This work was supported by the National Science Foundation under the grant ECS83-11987.

The authors are with the Department of Electrical and Computer Engineering, University of California, Santa Barbara, CA 93106.

IEEE Log Number 8607971.

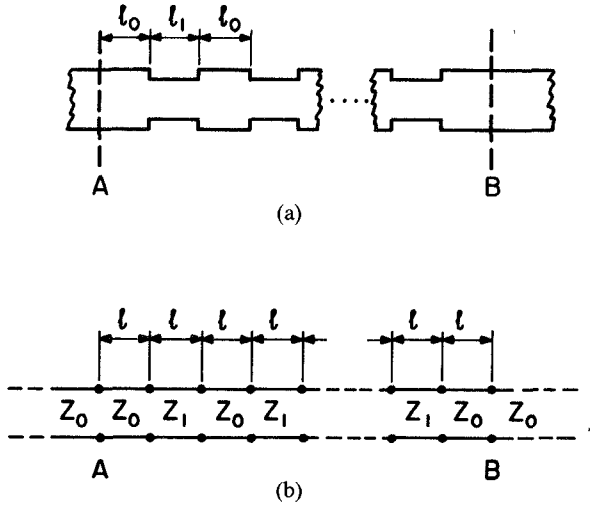

Fig. 1. (a) Top view of an image-guide grating. (b) An equal-line-length equivalent circuit for a grating such as that in (a).

length long. The grating impedance ratio is defined as

$$r = \frac{Z_1}{Z_0} > 1. \tag{1}$$

That the impedance ratio is larger than one for the type of gratings depicted in Fig. 1(a) has been confirmed by measurements. The two grating parameters f_0' and r are derived from tests made on a trial grating as we have discussed in [5]. The effects of dispersion on the frequency response are accounted for as discussed in the next paragraph and later in this paper. In [5] we also showed comparisons of measured and calculated frequency responses for some gratings demonstrating the accuracy of the model. Recently, there has also appeared completely theoretical analyses which predict the performance of dielectric image guide gratings [8].

An accurate model of DW gratings must include dispersion effects. Our approach has been to use a measured wave velocity at the center frequency, but the velocity is made to vary linearly as a function of frequency with a slope predicted by the effective dielectric constant (EDC) method [9]. Losses have been included in our model by using lossy transmission-lines with a loss per wavelength as has been measured for image guide at the frequency of interest.

Much in the same way, we model a pair of parallel-coupled gratings with a coupled, equal-line-length transmission-line circuit, as in Fig. 2. We assume that the gratings are coupled beginning from the middle of the first Z_0 section. The circuit is conveniently described in terms of its even- and odd-mode (i.e., the fields on the two gratings have either the same or opposite polarities, respectively). From experiments, we have learned that the effect of the coupling is to alter the odd- and even-mode wave velocities of the gratings while the impedances of the equivalent circuit remain almost unchanged from their uncoupled values except for very tight couplings. Note that this is consistent with the observation that image guide directional couplers are of the so-called "forward coupling"

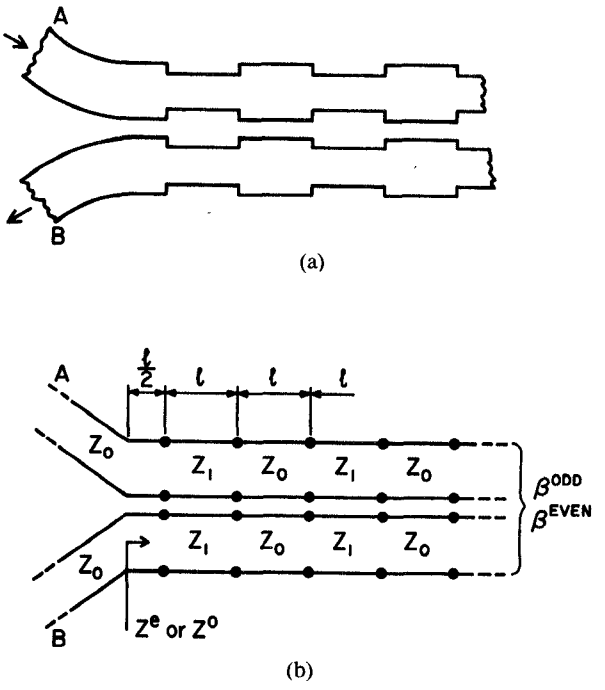

Fig. 2. At (a) is shown a pair of parallel-coupled gratings while at (b) is shown its equal-line-length, coupled transmission-line equivalent circuit.

type. Also, for simplicity, we use only one, average, odd- to even-mode velocity ratio to characterize a pair of coupled gratings, while in the actual grating, this ratio is different for the notched and unnotched regions.

III. Characteristics of Parallel-Coupled Gratings

The two-port transfer characteristics of parallel-coupled gratings, shown in Fig. 2(a), can be studied using the equivalent circuit in Fig. 2(b). It was shown in [5] that this circuit is completely described in terms of the impedances Z^e and Z^o that one sees looking into one of the gratings under even- and odd-mode excitation conditions, respectively. If the gratings are infinitely long and if Z^e and Z^o are defined in the middle of the first Z_0 section as in Fig. 2(b), they are the "image" impedances[1] of the grating and are given by [5]

$$Z^{e \text{ or } o} = Z_0 \sqrt{\frac{(1+r)\cos\Theta - (1-r)}{(1+r)\cos\Theta + (1-r)}} \tag{2}$$

where

$$\Theta = \Theta^e = \frac{\omega l}{v^e} \tag{3}$$

for the even mode and

$$\Theta = \Theta^o = \frac{\omega l}{v^o} \tag{4}$$

for the odd-mode, where v^e stands for the even-mode wave velocity and v^o stands for the odd-mode wave velocity. When (2) is imaginary, the sign for the square root must be

[1]A discussion of circuit image parameters will be found in [10, ch. 3].

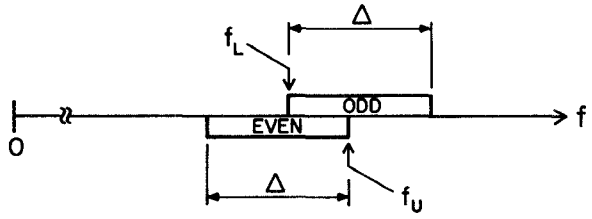

Fig. 3. The parallel-coupled gratings in Fig. 2 have odd- and even-mode stopbands located as shown above.

chosen so that the reactance versus frequency has a positive slope. Examination of the transfer function of the coupled gratings shows that the circuit behaves as a lossless circuit (line losses neglected) if *both* the even- and odd-modes of the gratings are in their respective stopbands i.e., if both Z^e and Z^o as given by (2) are purely reactive. So for the coupled gratings to behave as a lossless, reactive circuit between ports A and B in Fig. 2 over a band of frequencies, the odd- and even-mode stopbands must overlap as shown in Fig. 3. Each stopband has the same width because the impedance ratio is assumed to be the same for both modes, but they are shifted in frequency with respect to each other because the even- and odd-modes have different wave velocities. The fractional width of each image stopband was derived in [5] to be

$$\frac{\Delta}{f_0'} = \frac{4}{\pi}\sin^{-1}\left(\frac{r-1}{r+1}\right) \tag{5a}$$

where Δ is the stopband width. In an actual DW grating, dispersion will shrink the stopband bandwidth to be less than predicted by (5a). In narrow-band cases, a more accurate estimate can be obtained by dividing the bandwidth given by (5a) by [4], [5]

$$D = -\left[\frac{l_0\frac{d\lambda_{g0}}{df} + l_1\frac{d\lambda_{g1}}{df}}{l_0\frac{\lambda_{g0}}{f} + l_1\frac{\lambda_{g1}}{f}}\right]_{f=f_0} \tag{5b}$$

where l_0 and λ_{g0} are the length and wavelength for the Z_0 sections and l_1 and λ_{g1} for the Z_1 sections, respectively. This factor D also approximately predicts the effects of dispersion on the bandwidth of a complete filter and will be used for that purpose in Section V (see Sec. V, step 1). The width of the overlap band is most conveniently expressed as the ratio of its edge frequencies and can be shown to be

$$\frac{f_U}{f_L} = \frac{\cos^{-1}\left(\frac{1-r}{1+r}\right)}{\frac{v^o}{v^e}\cos^{-1}\left(\frac{r-1}{r+1}\right)}. \tag{6}$$

Parallel-coupled gratings, if properly designed, exhibit a transmission resonance behavior as was explained in [5] and [11]. They have a passband located within the overlap band and absorptive stopbands that can be very wide and strong. In the theoretical derivations, we have assumed that the gratings are infinitely long but finite length gratings

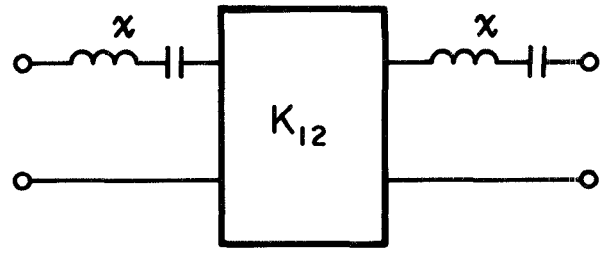

Fig. 4. An equivalent circuit that applies to the circuit of Fig. 1(b) near the center frequency of the grating stopband as well as to the circuit of Fig. 2(b) near the center frequency of the overlap band shown in Fig. 3.

can deliver almost the same performance as will be discussed later.

IV. Impedance Inverter Model of Gratings

It can be shown that both a single grating or a pair of coupled gratings can be modeled by the two-resonator equivalent circuit in Fig. 4 for frequencies in the vicinity of the grating stopband. This property was shown to hold for the uncoupled grating case in [12]. For the case of an impedance ratio r larger than one, the form with series resonators, as shown in Fig. 4, represents the grating between the reference planes A and B in Fig. 1(a). The equations giving the reactance slope parameter x and the impedance inverter parameter K_{12} in terms of the impedance ratio r and the number of Z_1 sections N are

$$K_{12} = Z_0\left(\frac{1}{r}\right)^N \tag{7a}$$

and

$$x = Z_0\frac{\pi\left[r - \left(\frac{1}{r}\right)^{2N}\right]}{4(r-1)}. \tag{7b}$$

For a general discussion and definitions of reactance slope parameters and impedance inverters see [10, ch. 4 and ch. 8]. Equations (7a,b) have been derived by generalizing results in [12]. (Also, here the equations have been written for a different choice of grating reference planes.)

In [5], the circuit of Fig. 4 was shown to also apply to coupled gratings with an impedance ratio larger than one, and equations were derived for the parameters of the circuit in Fig. 4. However, in [5] the formula for x required a numerical differentiation. Here we will take a slightly different point of view which will enable us to derive all the necessary expressions in closed form. Consider the two circuits shown in Fig. 5. We assume that in the circuit of Fig. 5(a) the lines are coupled beginning from the middle of the first Z_0 section. Reference planes are defined one eighth-wavelength from the coupled lines. In the analysis that follows, we make the simplifying assumption that the electrical length of these $\lambda/8$-lines is frequency independent. Since these line lengths are only $\lambda/8$ at f_0 and we are presently interested in parameters evaluated at f_0, this should cause little error.

The question arises as to what will fix the center frequency of the observed passband of the circuit in Fig.

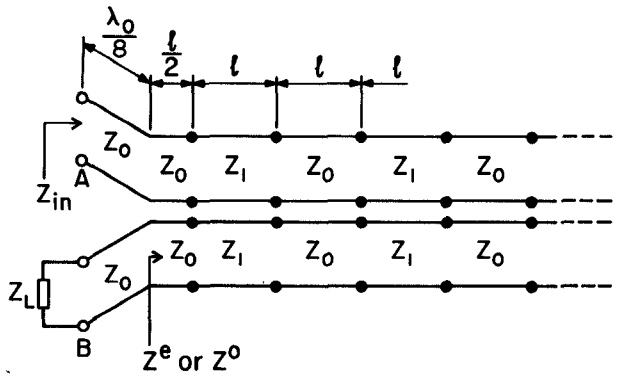

(a)

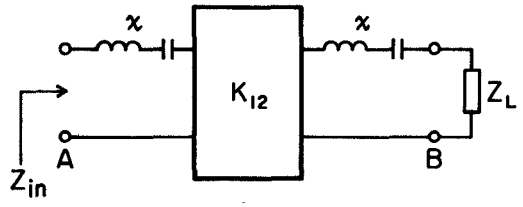

(b)

Fig. 5. An equivalent circuit for parallel-coupled gratings is shown at (a), while at (b) is shown a simplified equivalent for parallel-coupled gratings which applies at frequencies where the overlap-condition, shown in Fig. 3, is satisfied.

5(a). We can try to seek the answer from its impedance transforming properties. Use of standard circuit analysis shows that the input impedance seen, say, at port A when port B is terminated in an arbitrary load impedance Z_L is

$$Z_{in} = \frac{Z_0(X^e+X^o)Z_0 + Z_0(Z_0^2+X^eX^o) - jZ_L(Z_0^2-X^eX^o)}{Z_0(X^e+X^o)Z_L - Z_L(Z_0^2+X^eX^o) - jZ_0(Z_0^2-X^eX^o)} Z_0 \tag{8}$$

where X^e and X^o stand for the reactances seen looking into one of the gratings under even- and odd-mode conditions, respectively. In the case of infinitely long, lossless (or reasonably long, low-loss) gratings X^e and X^o can be computed from (2). Note that Z^e and Z^o are purely imaginary because at f_0 both modes are in their stopbands. The characteristic feature describing resonance in terms of impedance transforming properties of the circuit in Fig. 5(b) is that its input impedance is purely real at the center frequency if the load impedance is real. By (8) we find that for the circuit of Fig. 5(a) to behave similarly we must require that

$$X^eX^o = Z_0^2 \tag{9}$$

at the center frequency. If condition (9) is imposed on (8), it assumes a form similar to the familiar impedance-inverter relationship

$$Z_{in} = \frac{K_{12}^2}{Z_L} \tag{10}$$

where K_{12} is given by

$$K_{12}^2 = \frac{(X^e+X^o)+2Z_0}{(X^e+X^o)-2Z_0} Z_0^2. \tag{11}$$

It can be further simplified through the use of (9) to the form

$$K_{12} = Z_0 \left| \frac{Z_0+X^o}{Z_0-X^o} \right|_{f=f_0}. \tag{12}$$

The resonance condition (9) can also be written, through use of (2)–(4), as

$$\Theta^o|_{f=f_0} = \frac{\pi}{\frac{v^o}{v^e}+1}. \tag{13}$$

To derive an expression for the reactance slope parameter x of the resonator in Fig. 5(b), let Z_L be equal to jZ_0 and find the input reactance looking into port A in both cases. (An open circuit might seem to be a more logical choice for the load impedance, but choosing $Z_L = jZ_0$ leads to a simpler analysis in the case of Fig. 5(a).) Then take the derivative of the input reactance with respect to frequency in both cases and evaluate at f_0 as fixed by (9). Comparison of the resulting expressions will then allow one to find x. The calculations are somewhat lengthy, but straightforward, and details are omitted here. The result is

$$x = \frac{Z_0}{8}\Theta^o \left[\frac{X^o}{Z_0} f\left(\frac{v^o}{v^e}\Theta^o\right)\frac{v^o}{v^e} + \frac{Z_0}{X^o} f(\Theta^o) \right] \frac{\left[1-\left(\frac{K_{12}}{Z_0}\right)^2\right]^2}{1+\left(\frac{K_{12}}{Z_0}\right)^2} \tag{14}$$

where

$$f(\Theta) = \frac{(1+r)(1-r)\sin\Theta}{[(r+1)\cos\Theta-(r-1)]^2} \tag{15}$$

and X^e and X^o are obtained from (2), Θ^o from (13) and K_{12} from (12), all evaluated at f_0.

V. Bandpass Filter Design

Now we are going to illustrate the use of the foregoing concepts in the design of a bandpass filter. Consider the structure shown in Fig. 6(a). The overall effect of the gratings in this structure, and the resonance that occurs between two gratings adjacent in the same guide, is to form a two-resonator filter. The first resonator is formed by the resonance between gratings G_{01} and G_1 spaced a multiple of half guide wavelength apart. Its coupling to the input is controlled by the number of notches in grating G_{01}. Similarly, the second resonator is formed from gratings G_{23} and G_2 along with the line section between, and the coupling to the output is controlled by the number of notches in grating G_{23}. The coupling between the two resonators is controlled by the spacing between gratings G_1 and G_2. In the passband of the filter and in the immediately adjacent

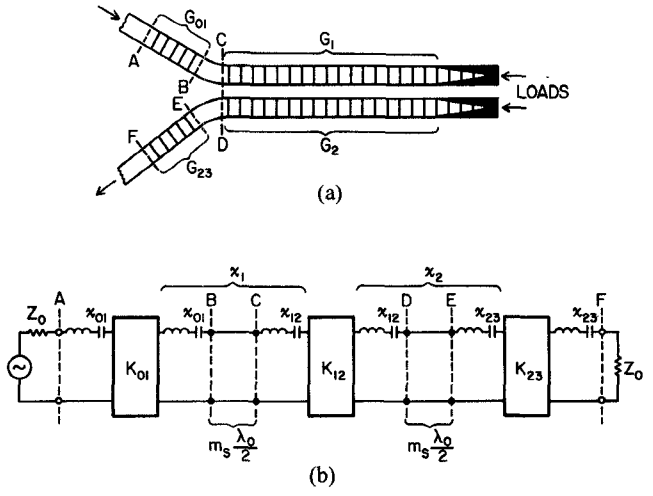

Fig. 6. (a) A two-resonator bandpass filter formed using DW gratings. (b) An equivalent circuit for the filter at (a) for frequencies in and near its passband.

portions of the filter stopbands, the gratings are reflecting strongly and very little power reaches the absorptive loads at the outer ends of the coupled gratings. Over this frequency band (where the gratings are in their stopband) the filter behaves much like a conventional reflection-type filter. Outside of that frequency range (where the gratings are in their passbands) the coupled gratings provide broad, absorptive stopbands for the overall filter in a manner as was discussed in [5] and [11]. The distributed loads at the outer ends of the coupled gratings are to absorb any power transmitted through the gratings with as low reflections as possible. On the other hand, the number of notches in the portion of gratings G_1 and G_2 which have no deliberately introduced losses are large enough so that very little power is lost to the grating loads in the passband of the filter. In this way, the performance of finite length parallel-coupled gratings differs very little from that of infinitely long gratings.

If the impedance inverter models of the coupled and uncoupled gratings are applied to the structure in Fig. 6(a), it is seen that in the vicinity of its center frequency it can be modeled as shown in Fig. 6(b), where the series L-C elements and the line sections m_s half-wavelengths long are all resonant at the same frequency f_0. The total reactance slope x_1 and x_2 of each resonator in Fig. 6(b) is the sum of the reactance slopes of its constituents. In this model, the role of the connecting waveguide between the gratings is simply to add

$$x_m = m_s \frac{\pi}{2} Z_0 \tag{16}$$

to the total reactance slope, where m_s is the number of half wavelengths in the connecting guide. The circuit in Fig. 6(b) is in a standard form to which direct-coupled-resonator filter theory [10, ch. 8] is readily applied permitting us to synthesize passband shapes such as Chebyshev or maximally flat characteristics. In doing this, the resonator element on the far left with slope parameter x_{01} and the resonator element on the far right with parameter x_{23} are ignored. This is justified because x_{01} and x_{23} are relatively small.

Before going into a detailed design procedure, we make some general comments. First, it is often desirable to design filters such as in Fig. 6 so that the resulting structure will be symmetrical. This will be feasible when using typical Chebyshev or maximally flat prototypes which are symmetric or antimetric (see [10, Sec. 4.05]). Therefore, we assume that gratings G_{01} and G_{23} are identical. Second, in all the design examples we have considered, we have found that it is simplest to have the same amount of frequency selectivity in each resonator. Therefore, the filter will be designed so that the total reactance slope parameter of both resonators is the same. Finally, we assume that the designer has appropriate data available so that the effective impedance ratio of the gratings to be used and their center frequency are known. Means for getting such data were discussed in [5].

For convenience, some of the equations from [10] are repeated here. In [10] the filter designs are derived from normalized low-pass prototypes with element values $g_0, \cdots, g_{n+1}$ and low-pass cutoff frequency ω_1'. With reference to Fig. 6(b), we have

$$K_{01} = \sqrt{\frac{R_A x_1 w}{g_0 g_1 \omega_1'}} = K_{23} \tag{17a}$$

$$K_{12} = \frac{w}{\omega_1'} \sqrt{\frac{x_1 x_2}{g_1 g_2}} \tag{17b}$$

where w is the fractional bandwidth of the filter and $R_A = Z_0$ in the case of Fig. 6(b). The design proceeds as follows:

1) Select a low-pass prototype [10, ch. 4] and find the bandwidth that should be used in the design by multiplying the desired filter bandwidth by D, given by (5b), in order to compensate for dispersion.

2) Choose the overlap bandwidth of the stopbands of the coupled gratings. It should be larger than the design bandwidth of the filter because the equivalent circuit of Fig. 4 applies only at frequencies where the even- and odd-mode stopbands overlap as shown in Fig. 3. Therefore, the overlap band should include the passband and a small part of the filter stopband on each side. On the other hand, too large an overlap bandwidth implies a smaller odd- to even-mode velocity ratio, hence larger spacing between the gratings and looser coupling. The end result of this is that the bandwidth desired for the filter may not be realizable. More will be said about this later. For the overlap bandwidth chosen, determine f_U/f_L (see Fig. 3) and solve for the v^o/v^e required by use of (6).

3) Now we have fixed the parameters of the coupled gratings. Use (12) and (14) to find the impedance inverter parameter of the coupled gratings K_{12} and the associated reactance slope parameter x_{12}.

4) Insert the value of K_{12} into (17b) and solve for x_1 and x_2 assuming they are equal.

5) Insert x_1 from above into (17a) and find what is the required value of K_{01}.

6) Use (7a) to find what is the number of notches required in the grating G_{01} by finding the integer value of N which will give K_{01} closest to the value desired.

7) Use (7b) to find the reactance slope parameter x_{01} of the grating G_{01}.

8) The total reactance slope of each resonator is

$$x_1 = x_{12} + x_{01} + m_s \frac{\pi}{2} Z_0 \tag{18a}$$

$$x_2 = x_1 = x_{12} + x_{23} + m_s \frac{\pi}{2} Z_0 \tag{18b}$$

where m_s is the number of half wavelengths in the connecting waveguide in each resonator. The design is completed by choosing an integer value for m_s such that x_1 is closest to the value that the design calls for in step 4.

If the resulting value for m_s or the number of notches is not convenient, then the procedure may be repeated for a different choice of overlap bandwidth or a different impedance ratio, if that is available. Although presented here only for the case of a two-resonator filter, as will be discussed later, the procedure is applicable to the design of four- or six,- etc., resonator filters.

So far we have neglected the additional resonators to the left of K_{01} and to the right of K_{23} in Fig. 6(b). Often, ignoring them completely is a good approximation because they are so heavily loaded by the input and output terminations that their contribution to the overall frequency response is indeed negligible. Also, in most cases, the overall frequency response tends to be somewhat distorted anyway because of the various approximations involved. In particular,we have found that the equal-ripple bandwidth is almost always a little larger than the design bandwidth, and the ripple size cannot always be exactly as chosen. One notable reason for this is that the parameters of the gratings can only be adjusted in discrete steps (the number of notches in a grating has, of course, to be an integer).

VI. Bandwidth Limitations

As was implied earlier, there are limitations to the maximum passband bandwidth that is available in this kind of filter. The first limitation comes from the fact that the equivalent circuit of Fig. 4 applies only at frequencies where the stopbands of the coupled gratings overlap as shown in Fig. 3. The overlap bandwidth can be increased by decreasing the odd- to even-mode velocity ratio, but this implies larger spacing between the gratings and hence looser coupling. In the limit, the odd- and even-mode stopbands can completely overlap each other, but then, of course, there is no coupling at all. Therefore, for a given grating impedance ratio r, there is some value of odd- to even-mode velocity ratio (i.e., a spacing between the gratings) for which there is the maximum amount of potential filter bandwidth available. If, in the design procedure stated before, the overlap bandwidth has been specified to be too large and therefore the coupling between the gratings is too loose for a desired filter bandwidth, it will manifest itself in that in step 8 of the procedure, the required left-hand side of (18a,b) will be smaller than the right-hand side even if we set $m_s = 0$. If at this point reducing the overlap bandwidth would make that bandwidth to be smaller than (or almost equal to) the desired passband width of the filter, then the only recourse available is to use a larger grating impedance ratio.

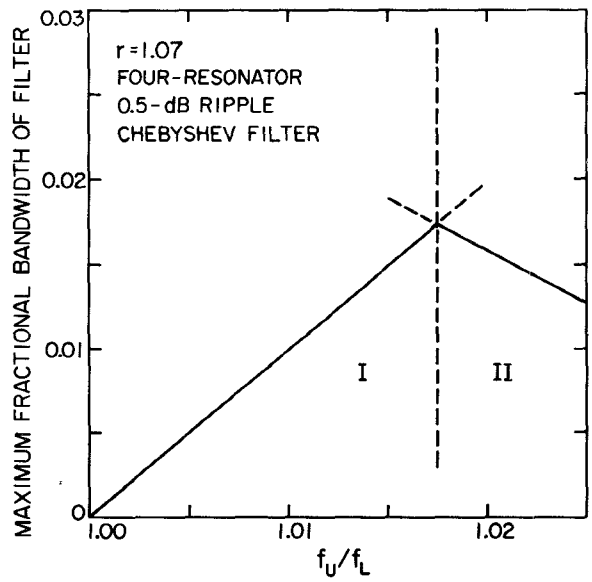

Fig. 7. The maximum available passband width of the filter is shown as a function of the ratio f_U/f_L of the edge frequencies of the overlap band (see Fig. 3). In region I of this graph, the available filter bandwidth is limited by the width of the overlap band while in region II the coupling between the parallel-coupled gratings becomes so loose that it limits the amount of filter bandwidth that can be realized.

No general statements about the maximum bandwidth or the optimum odd- to even-mode velocity ratio for a given impedance ratio can be made because the choice of these parameters is influenced by the low-pass prototype chosen. In Fig. 7, we illustrate the bandwidth limitations for the case of an impedance ratio $r = 1.07$ while using a 0.5-dB ripple, four-resonator, Chebyshev low-pass prototype. Shown there is the maximum available bandwidth of the filter as a function of the ratio of the edge frequencies of the overlap band with the assumption that in the limit we can take $m_s = 0$ in (18a, b), which may lead to impractical structures but serves to indicate a theoretical limit.

VII. Design Example and Experimental Results

Two- and four-resonator filters based on the principles presented above have been built and tested. Experimental results for a trial two-resonator design were presented in [5]. In [5] we also proposed a three-resonator version in which all three resonators were placed side-by-side to provide coupling between them. Such a filter was subsequently designed and tested, but the experimental results did not give as strong stopbands as we had expected. In order to achieve as strong stopbands as possible, we concluded it is preferable to use structures having directly connected grating couplings alternating with parallel-grating couplings, as in the four-resonator structure in Fig. 8. Note that this structure uses three directly connected coupling gratings G_{01}, G_{23}, and G_{45}, and two sets of parallel-

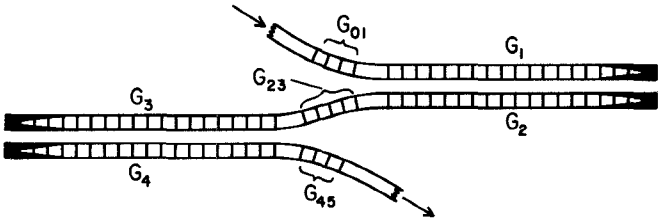

Fig. 8. A four-resonator filter formed using DW gratings.

coupled gratings. Since the decibel attenuations due to the absorptive stopbands of the parallel-coupled gratings (terminated in loads) add, the potential stopband attenuation of the filter is very high.

A trial four-resonator filter was designed using a design procedure similar to the one presented above for the two-resonator case. In an earlier work [5], we had studied DW image guide gratings using Rexolite 1422 having $\varepsilon_r = 2.55$ and had found that for some convenient dimensions the effective impedance ratio was 1.07. We chose to use those gratings for this design. A 0.5-db Chebyshev ripple low-pass prototype was chosen. The prototype element values are [10, ch. 4]

$$g_0 = 1 \quad g_1 = 1.6703 \quad g_2 = 1.1926$$
$$g_3 = 2.3661 \quad g_4 = 0.8419 \quad g_5 = 1.9841$$

with $\omega_1' = 1$. The design bandwidth was set at 1.5 percent without dispersion correction. Computing the factor D given by (5b), we found D equals 1.37 for the dimensions of our gratings at the center frequency, so the actual bandwidth of the filter was expected to be about 1.1 percent. The derivatives in (5b) were found by use of the EDC method [9]. The ratio of the edge frequencies of the overlap band of the coupled gratings was chosen to be 1.02. Then the required v^o/v^e is found to be 1.024. By (13) Θ^o is 1.552 at the center frequency and by (2) X^o is $-1.871Z_0$. The impedance-inverter parameter of the coupled gratings is by (12) $K_{12} = 0.3035Z_0 = K_{34}$ and the associated reactance slope parameter is from (14) $x_{12} = 15.20Z_0 = x_{34}$. Then from step 4 we get $x_1 = x_2 = x_3 = x_4 = 28.56Z_0$. Following step 5 we compute $K_{01} = 0.5064Z_0 = K_{45}$ and $K_{23} = 0.2550Z_0$. Using (7a), the closest integer values of N yielding the required inverter parameters are $N_{01} = N_{45} = 10$ for gratings G_{01} and G_{45} and $N_{23} = 20$ for grating G_{23}. The corresponding reactance slopes are from (7b) $x_{01} = x_{45} = 9.106Z_0$ and $x_{23} = 11.26Z_0$. Finally we can conclude that we should use $m_s = 3$ half-wavelengths of connecting guide between gratings G_{01} and G_1 and $m_s = 1$ half-wavelengths between G_2 and G_{23}.

In Fig. 9, we show a calculated frequency response for the design presented above. In Fig. 9, dispersion and line losses have been taken into account. The response was calculated assuming a line loss of 0.0227 dB per guide wavelength which was based on loss measurements of image guide at the frequency of interest. Bandwidth is difficult to define for the response shown because the shape of the passband is rounded due to losses. If the same response is calculated for the lossless case, equal-ripple

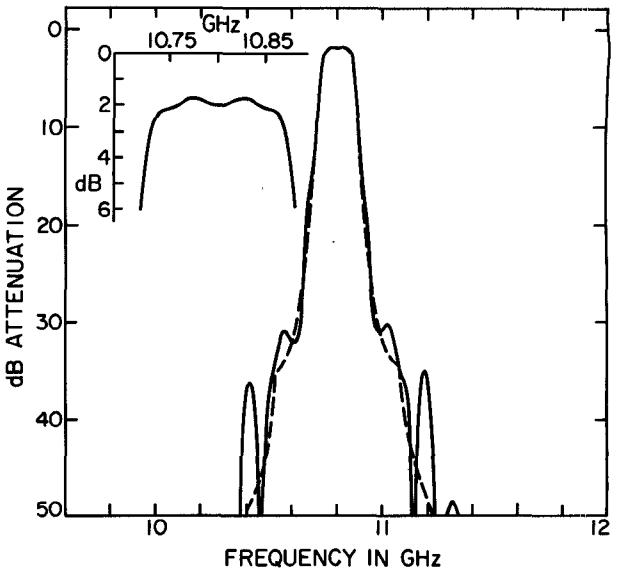

Fig. 9. The solid line shows a computed response for a four-resonator DW filter as shown in Fig. 8 with distributed loads at the outer ends of the parallel-coupled gratings, while the dashed line shows the corresponding response with infinite, parallel-coupled gratings.

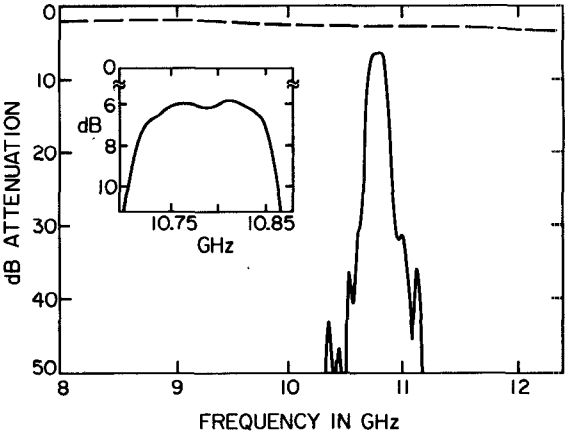

Fig. 10. A measured response for a four-resonator filter as in Figs. 8 and 9. The dashed line indicates the loss due the mode launchers and the lengthy input and output guides that were used.

bandwidth is found to be 1.2 percent including the effects of dispersion. In Fig. 9, the dashed line shows the stopband response for the case of the coupled gratings being infinitely long while the solid line shows the corresponding response with coupled gratings having 68 notches. Twenty-one of these notches belong to the distributed load. In these calculations the loss in the distributed load was linearly increased up to 2.3 dB per guide wavelength, and then the last line section was terminated in a lumped Z_0 load.

A corresponding experimental filter was fabricated, and its measured frequency response is shown in Fig. 10. The test set up used some fairly lengthy input and output guides to the filter, and the dashed line in Fig. 10 indicates the loss due to these lines and mode launchers. The mid-band loss of the filter alone is about 3.1 dB which is somewhat higher than expected. We believe this is due to

radiation from some relatively sharp bends used in this filter. In general we have found that sharp bends would be desirable in order to separate the coupled gratings as rapidly as possible at their input end, but bends with a small radius of curvature tend to radiate, as is well known. To get the response shown in Fig. 10, the filter was fine tuned by adjusting the spacing between the coupled gratings to realize the required v^o/v^e and small pieces of dielectric were placed near the center of the resonators to bring them all to resonance at the same frequency.

Measurements were made of the stopband up as far as 26.5 GHz. In the 12- to 18-GHz range, except for two frequencies, the attenuation was in excess of 55 dB provided that metal or absorbing dividers were put between the input and output guides and the adjacent gratings. These walls were found to be desirable to suppress stray coupling between gratings, e.g., between G_{01} and G_{23} in Fig. 8. At the two frequencies mentioned, the attenuation dropped to 37 and 45 dB. It was found experimentally that the attenuation at these two weak points could be increased above 55 dB if several pieces of fine metal wire were placed transverse to the guide axis on top of the G_{23} grating in Fig. 8. These wires did not affect the rest of the response. We believe the observed weak points and their disappearance with the wires is due to higher-order modes of the DW. In the 18- to 26.5-GHz range, attenuation was in excess of 55 dB except for one frequency where it dropped to 47 dB, again provided that the dividers were in place. This 47 dB could not be further suppressed with the wires. We also made tests with no measures taken to suppress stray couplings or higher order modes. Even then the typical attenuation was 50 dB in the 12- to 18-GHz range and 40 dB in the 18- to 26.5-GHz range, with a 37-dB minimum stopband attenuation in the full 8- to 26.5-GHz range measured, so the stopband performance of this type of filters is inherently good.

VIII. Conclusions

Techniques for the design of bandpass filters using dielectric waveguide gratings have been presented. These filters use both uncoupled gratings and parallel-coupled configurations of gratings. Simple transmission-line equivalent circuits have been used to analyze these structures. It was shown how direct-coupled-resonator filter theory can be applied to design two-, four-, six-, etc., resonator-filters which have Chebyshev, maximally flat, or other passband characteristics. Meanwhile, the use of gratings in a parallel-coupled configuration gives these filters their broad, strong stopband characteristics. These filters are capable of high stopband attenuations over a broad band of frequencies, and the attenuation is absorptive over most of the stopband which should be an additional advantage. The passband width is limited to less than perhaps, a few percent in most cases, and the reasons for this were discussed. Experimental results for a four-resonator filter were presented and they agreed well with theoretical calculations. Experiments were carried out using dielectric image guide, but the design technique itself is applicable to other forms of waveguides as well.

References

[1] R. M. Knox, "Dielectric waveguide microwave-integrated circuits—An overview," *IEEE Trans. Microwave Theory Tech.*, vol. MTT-24, pp. 806–814, Nov. 1976.

[2] T. Yoneyama, F. Kuròki, and S. Nishida, "Design of nonradiative dielectric waveguide filters," *IEEE Trans. Microwave Theory Tech.*, vol. MTT-32, pp. 1659–1662, Dec. 1984.

[3] T. Itoh, "Applications of gratings in a dielectric waveguide for leaky-wave antennas and band-reject filters," *IEEE Trans. Microwave Theory Tech.*, vol. MTT-25, pp. 1134–1138, Dec. 1977.

[4] D. C. Park, G. L. Matthaei, and M. S. Wei, "Bandstop filter design using a dielectric waveguide grating," *IEEE Trans. Microwave Theory Tech.*, vol. MTT-33, pp. 693–702, Aug. 1985.

[5] G. L. Matthaei, D. C. Park, Y. M. Kim, and D. L. Johnson, "A study of the filter properties of single and parallel-coupled dielectric-waveguide gratings," *IEEE Trans. Microwave Theory Tech.*, vol. MTT-31, pp. 825–835, Oct. 1983.

[6] G. L. Matthaei, "A note concerning modes in dielectric waveguide gratings for filter applications," *IEEE Trans. Microwave Theory Tech.*, vol. MTT-31, pp. 309–312, March 1983.

[7] E. A. J. Marcatili, "Dielectric rectangular waveguide and directional coupler for integrated optics," *Bell Syst. Tech. J.*, vol. 48, pp. 2071–2102, Sept. 1969.

[8] H. Shigesawa, M. Tsuji, and K. Takiyama, "Microwave network representation of discontinuity in open dielectric waveguides and its applications to periodic structures," in *1985 IEEE MTT-S Int. Microwave Symp. Dig.*, pp. 623–626.

[9] W. V. McLevige, T. Itoh, and R. Mittra, "New waveguide structures for millimeter-wave and optical integrated circuits," *IEEE Trans. Microwave Theory Tech.*, vol. MTT-23, pp. 788–794, Oct. 1975.

[10] G. L. Matthaei, L. Young, and E. M. T. Jones, *Microwave Filters, Impedance-Matching Networks, and Coupling Structures*. New York: McGraw-Hill, 1964; Dedham, MA: Artech House, 1980.

[11] P. K. Ikäläinen, G. L. Matthaei, D. C. Park, and M. S. Wei, "Dielectric waveguide bandpass filters with broad stopbands," in *1985 IEEE MTT-S Int. Microwave Symp. Dig.*, pp. 277–280.

[12] G. L. Matthaei, E. B. Savage, and F. Barman, "Synthesis of acoustic-surface- wave-resonator filters using any of various coupling mechanisms," *IEEE Trans. Sonics Ultrason.*, vol. SU-25, pp. 72–84, Mar. 1978.

✠

Pertti K. Ikäläinen (S'86) was born in Pieksämäki, Finland, on Feb. 3, 1957. He received the Diploma Engineer (M.Sc.) degree in electrical engineering from the Helsinki University of Technology, Espoo, Finland, in 1981.

In 1980, he joined the Technical Research Center of Finland, Telecommunications Laboratory. Since 1983, he has been on leave from his position there to pursue the Ph.D. degree at the University of California, Santa Barbara, as a Fulbright scholar. His current research interests are in the area of waveguide components for millimeter-wave applications using dielectric waveguides.

George L. Matthaei (F'65) received the B.S. degree from the University of Washington in 1948 and the Ph.D. degree from Stanford University in 1952.

From 1951 to 1955, he was on the faculty of the University of California, Berkeley, where he was an Assistant Professor, and his specialty was network synthesis. From 1955 to 1958, he was engaged in system analysis and microwave component research at the Ramo-Wooldridge Corporation. From 1958 to 1964, he was at the Stanford Research Institute where he was engaged in microwave device research and became Manager of the Electromagnetic Techniques Laboratory in 1962. In July 1964, he joined the Department of Electrical Engineering at the University of California, Santa Barbara, where he is a Professor. He is the author of numerous papers, coauthor of the book *Microwave Filters, Impedance-Matching Networks, and Coupling Structures*, and a contributor to several other books.

Dr. Matthaei is a member of Tau Beta Pi, Sigma Xi, and Eta Kappa Nu. He was the winner of the 1961 Microwave Prize of the IEEE MTT Group and is a recipient of an IEEE Centennial Medal.